

Analysis on FM-to-AM conversion induced by spatial filter in a high-power laser system

Hujie Zhang (张琥杰)^{1*}, Shenlei Zhou (周中蕾)¹, Youen Jiang (姜有恩)¹, Jinghui Li (李菁辉)¹, Wei Feng (冯伟)², and Zunqi Lin (林尊琪)¹

¹National Laboratory on High Power Laser and Physics, Shanghai Institute of Optics and Fine Mechanics, Chinese Academy of Sciences, Shanghai 201800, China

²Shanghai Institute of Laser and Plasma, Shanghai 201800, China

*Corresponding author: zhanghujie@ustc.edu

Received October 12, 2011; accepted December 12, 2011; posted online February 20, 2012

In order to avoid stimulated Brillouin scattering and smooth the final focal spot that reaches the D-T capsule, spectral broadening is essential. However, the modulation of spectral structure might result in frequency-to-amplitude modulation (FM-to-AM) conversion. The spatial filter pinhole is used to cut off the high-frequency transmission laser, and to ensure the desired pass. Improper parameter of pinhole would lead a negative impact. Using the spatial filter pinhole, we analyze the characteristic of intensity modulation using several pinholes of improper parameters. We then compare these results with the intensity modulation obtained from an experiment. Experimental diagnosis and design of an appropriate pinhole parameter would be highly beneficial to the field of high-power lasers.

OCIS codes: 050.5080, 070.2615, 220.4840, 300.1030.

doi: 10.3788/COL201210.060501.

To ensure the stability of implosion experiment in ICF, a high-quality temporal pulse shape laser is necessary. Some problems, such as how to control temporal profile and frequency-to-amplitude modulation (FM-to-AM) conversion^[1], must be studied in detail. In the high-power laser system, the laser spectrum is broadened for two reasons to avoid stimulated Brillouin scattering^[2] (SBS) and to “smooth” the final focal spot that reaches the D-T capsule. First, without spectral broadening, spectral power density of ignition laser pulses would exceed the transverse Brillouin threshold in optics at the end of the amplifier chain, thereby severely damaging the optics components. Spectral broadening spreads energy to different wavelengths to reduce the spectral power density maximum level below the SBS threshold. Second, nonuniformities in the laser irradiation may seed the Rayleigh-Taylor hydrodynamic instability, which degrades target performance. Therefore, high spatial homogeneity^[3] is desired for focal spots. In fact, the focal spot of the laser beam is shaped by a phase plate and appears as a speckle pattern with hot spots. The intensity is time-averaged through spectral broadening and a dispersion system (grating) that moves the hot spots during the pulse. This scheme is called smoothing by spectral dispersion^[4].

Although the required spectral broadening adopted by the aforementioned techniques are generated by a pure phase modulation that would not impact the spatial intensity distribution directly, some optical components, including fibers, amplifier media, and spatial filters, could slightly affect the spectrum. The consequences of such filters are a partial conversion of FM into intensity modulation called FM-to-AM conversion. Hocquet and Yang analyzed the factors resulting in FM-to-AM conversion in detail, including group velocity dispersion, gain narrowing, frequency doubling, grating, and so on^[5-7]. Unfortunately, to the best of our knowledge, the conver-

sation induced by the sideband cutoff of a spatial filter pinhole has not yet been discussed. Spatial filter is a necessary element in high-power laser systems, undertaking beam expanding, image transferring, filtering, and so on. In the present letter, we mainly analyze the FM-to-AM conversion induced by spatial filter. The obtained results can be used for the design of a spatial filter in a high-power laser system.

FM-to-AM conversion is an intensity modulation induced by phase modulation. It results in a spiking oscillation on the temporal shape, which would affect the laser beam quality and reduce the safety operation energy.

FM-to-AM conversion is rooted in the transmission inhomogeneity of broad spectrum, and would lead to spectrum distortions, including amplitude and phase distortions. The distortion criterion α , called the FM-to-AM conversion factor, has been defined as^[8]

$$\alpha = 2 \frac{P_{\max} - P_{\min}}{P_{\max} + P_{\min}}, \quad (1)$$

where P_{\max} and P_{\min} are the maximum and minimum optical powers over one phase modulation period, respectively. Here, α ranges from 0% to 200% and is ideally equal to 0.

Considering a transmission system with a following intensity filtering function^[9]

$$H(f) = 1 - \sigma_f(f - f_c)^2, \quad (2)$$

where f_c is the central frequency of the filter and σ_f is the filtering coefficient.

Because sinusoidal phase modulation is always adopted, the modulated optical field can be given by

$$a_0(t) = \exp[i\delta \sin(2\pi f_m t)], \quad (3)$$

where δ is the modulation depth and f_m is the modulation frequency.

The output intensity can then be calculated as

$$I_{\text{out}}(t) \approx 1 - \sigma_f [f_c - \delta f_m \cos(2\pi f_m t)]^2. \quad (4)$$

The period of the intensity modulation is the same as that of the phase modulation, except when $f_c = 0$. When f_c equals zero, Eq. (4) can be rewritten as

$$I_{\text{out}}(t) \approx 1 + \sigma_f (\delta f_m)^2 [1 + \cos(4\pi f_m t)]/2. \quad (5)$$

From Eq. (5), we can deduce that the period of the intensity modulation would be equal to the half period of the phase modulation.

On condition that f_c is smaller than δf_m , f_c can be ignored. When it is much smaller than δf_m , the FM-to-AM conversion factor is given by

$$\alpha = \frac{\sigma_f (f_c + \delta f_m)^2}{1 - \frac{1}{2} \sigma_f (f_c + \delta f_m)^2}. \quad (6)$$

When f_c is larger than δf_m , α is given by

$$\alpha = \frac{4\sigma_f \delta f_m f_c}{1 - \sigma_f (f_c^2 + \delta^2 f_m^2)}. \quad (7)$$

The analysis above refers to the case in which FM-to-AM conversion is induced by an amplitude mismatching. As each spectrum obtains a different gain or attenuation, the relative intensity of each spectra changes and FM-to-AM conversion occurs. In addition, phase mismatching causes FM-to-AM conversion due to the different phase delay of each spectrum^[10], such as a spiking oscillation caused by the beat effect of mismatching spectra, the frequency of intensity modulation would be equal to frequency difference of beat frequency. Because the FM-to-AM conversion caused by an improper parameter pinhole belongs to the situation of intensity mismatching, phase mismatching is not be discussed in detail in the present letter.

In the SSD experiment, as shown in Fig. 1^[11], the incident beam is spectrally broadened by an electro-optic modulator. The beam is then dispersed by a grating to realize spatial dispersion. Finally, the spot transfers rapidly on the focal plane to smooth the random high-frequency region of asymmetric intensity.

A sinusoidal phase modulation is induced, the main parameter includes The modulation frequency f_m and the modulation depth δ .

The optical field incident beam can be expressed as

$$E_0(t) = A_0(t) \exp(i\omega_0 t), \quad (8)$$

where $A_0(t)$ is the temporal envelope of the incident beam and ω_0 is the circular frequency of the beam.

By expanding by the modulator, the optical field becomes

$$E_M(t) = A_0(t) \exp\{i[\omega_0 t + \delta \sin(2\pi f_m t)]\}. \quad (9)$$

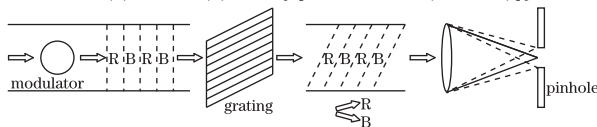


Fig. 1. Schematic of the SSD system.

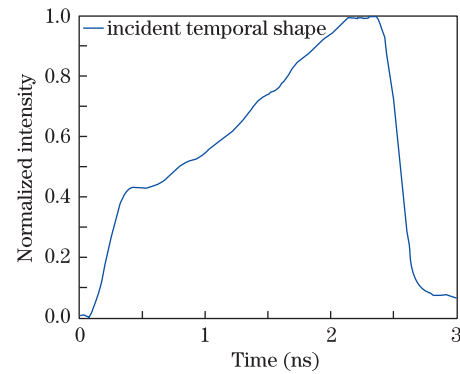


Fig. 2. Temporal shape of the incident beam.

One can express the beam-smoothing problem as a Fourier transform:

$$A(f) = A_0 \sum_{n=-\infty}^{\infty} J_n(\delta) \delta(f - n f_m), \quad (10)$$

where $J_n(\delta)$ is the n th order of the Bessel function. In theory, the spectrum structure has an infinite bandwidth; however, because of the character of the Bessel function, the energy of the side frequency attenuates rapidly. In fact 98% of the energy is centralized within $2(m+1)f_m$.

The spectrally dispersed beam is then spatially dispersed by a grating in the x direction. The optical field can be described by

$$E_G(x, t) = A_0 e^{i[\omega_0 t + \delta \sin \omega_m t - (\omega_t/c)x \sin \theta]}, \quad (11)$$

where instantaneous frequency $\omega_t = \omega_0 + 2\pi\delta f_m \cos(2\pi f_m t)$, the corresponding instantaneous dispersion angle $\theta = \frac{\Delta\theta}{\Delta\lambda} \frac{\lambda}{\omega_0} (\omega_t - \omega_0)$.

Because the spatial filter pinhole localizes at the far field of the laser system the distribution at the pinhole can be obtained by a Fourier transform:

$$E(u, t) = T(x) \text{FFT}([E_G(x, t)]), \quad (12)$$

where $E(u, t)$ is the distribution at the focal plane at time t and $T(x)$ is the transmission function of pinhole.

$$T(x) = \begin{cases} 1, & x < \text{radius} \\ 0, & x > \text{radius} \end{cases}. \quad (13)$$

The intensity could be calculated by integrating

$$I(t) = \int |E(u, t)|^2 du. \quad (14)$$

An improper parameter of pinhole can significantly affect the FM-to-AM conversion. First, a pinhole with an insufficient size would partially cut off necessary high-frequency components. Second, shifting of the central wavelength will shift the central position of the pinhole, thereby cutting off the high-frequency components asymmetrically. Finally, if the pinhole localizes at a defocused plane at a quasi-near-field location, the dispersed spot would be cut off and each spectrum would have a different intercepting factor. All the situations mentioned above lead to FM-to-AM conversion; however, some differences evident among these temporal aberrances will be analyzed particularly in the following section.

Assuming that a sinusoidal modulation of modulation frequency of 3 GHz and a depth of 5 is adopted, the engraved lines of a dispersion grating is 1 480 per mm, the beam aperture D is 30 mm, the central wavelength of the laser λ is 1 053 nm, and the focal length of lens f is 1255 mm, the diffraction limits would be

$$DL = 1.22 \frac{\lambda f}{D}. \tag{15}$$

The near-field divergence angle of each sideband could be calculated by

$$\Delta\theta = \frac{\Delta\theta}{\Delta\lambda} \frac{\lambda}{\omega_0} n\omega_n, \tag{16}$$

whereas the spreading distance of the corresponding far field located at the spatial filter pinhole should be

$$\Delta l = f\Delta\theta. \tag{17}$$

The grating dispersion $\frac{\Delta\theta}{\Delta\lambda}$ is 2.36 mrad/nm, ω_0 is the corresponding central angular frequency, ω_n is the modulation angular frequency, and f is the focal length. Substituting these parameters into Eqs. (15)–(17), we obtain

$$DL = 53.7 \mu\text{m}, \tag{18}$$

$$\Delta l = n \cdot 26.2 \mu\text{m}, \tag{19}$$

where n is the order number of sideband.

The temporal shape of the incident beam is shown in Fig. 2.

When the diameter of aperture is 483 μm , which is nine times the diffraction limit, the temporal shape at this condition can be calculated from Eqs. (11), (12), and (14), as shown in Fig. 3.

In Fig. 3, the dotted line represents the incident temporal shape, whereas the solid line represents the modulated temporal shape. Under this condition, the aperture is sufficiently large that the field from the ± 1 st to ± 9 th side lobe can all pass through the pinhole; therefore, no intensity modulation can be found.

To reveal the relationship between the FM-to-AM conversion and the pinhole size, we reduce the aperture 52 μm each time and record the corresponding temporal shape, as shown in Fig. 4.

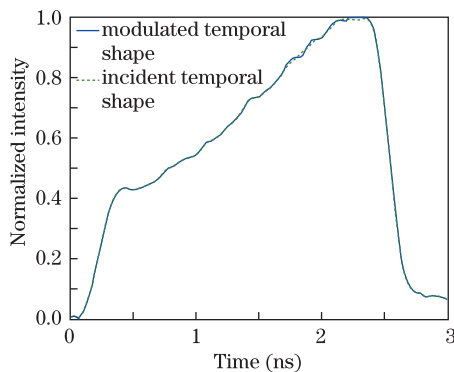


Fig. 3. Temporal shapes of input and output beams under a pinhole of 9 DL.

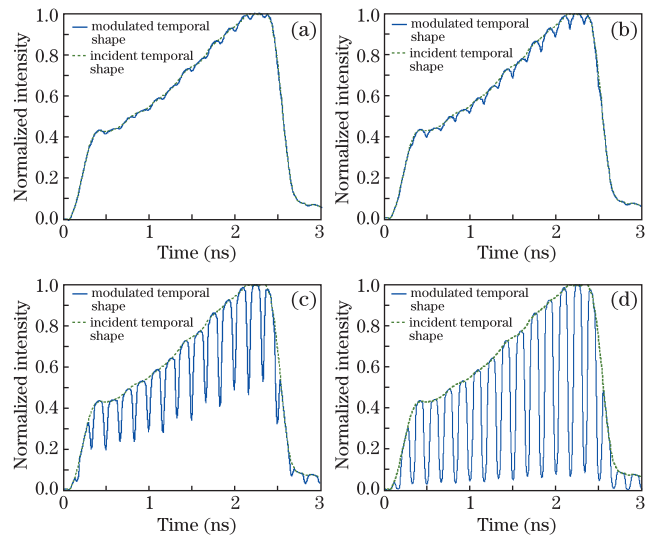


Fig. 4. Temporal shapes of input and output beams under pinholes with different diameters of (a) 431, (b) 379, (c) 327, and (d) 275 μm .

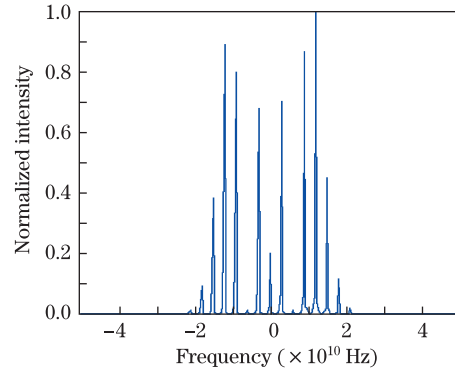


Fig. 5. Energy distribution of each sideband.

With the reduction of the pinhole size, the resulting intensity modulation is enlarged. As the pinhole reduces, more sidebands are cut off. Due to the character of Bessel function, the energy distributed on each sideband is inhomogeneous, which is the reason for the distortion criterion nonlinearity. As shown in Fig. 4, the intensity modulation period is 0.17 ns, which is half of the phase modulation period $f_c=0$ mentioned in Eq. (13) for the symmetry of intensity-filtering function.

Furthermore, the energy distribution at each sideband is studied to determine the relationship of the intensity filtering function and intensity modulation. The energy power is related to the character of Bessel function, as shown in Fig. 5.

When the aperture diameter is 483 μm , which is nine times the diffraction limits, all ± 9 sidebands pass through the pinhole. Meanwhile, energy of the 10th order sideband cut off by pinhole is barely identifiable. Under this condition, no modulation at this condition, and FM-to-AM conversion shown in Fig. 3 would not occur. When the aperture becomes reduced to 431 μm , the ± 8 th sideband passes through the pinhole. Although the 9th order sideband cannot be identified from Fig. 5, the slight FM-to-AM conversion is sensitive to the spectra modulation in Fig. 4(a). When the aperture becomes reduced to 379 μm , the ± 7 th sideband would

pass through. However, the 8th order sideband remains weak, and intensity modulation with a low distortion criterion can be found (see Fig. 4(b)). Similarly, when the aperture becomes reduced to 327 μm , the ± 6 th sideband passes through, and the 7th sideband can be clearly observed. A high-intensity modulation is realized in the corresponding Fig. 4(c). Finally, when the aperture becomes reduced to 275 μm , only the ± 5 th sideband is able to pass through, and a severe spectrum distortion results in a significant FM-to-AM conversion, as shown in Fig. 4(d).

At the SSD experiment, shifting of the central wavelength will result in the shift of center spectrum through dispersion grating whose mathematic model is the same as off-axis. We could consider the shifting distance of center spectrum as the off-axis distance. Under this condition, although the aperture size satisfies the requirements mentioned in Fig. 4(a), several sidebands would be cut off, thereby leading to FM-to-AM conversion.

In order to show the difference between Figs. 4 and 6, we calculate the temporal shape to illustrate the character of the off-axis.

The aperture diameter is kept at 483 μm . As the pinhole shifts, several spectra will be cutoff asymmetrically. As shown in Fig. 6, when the pinhole shifts along the positive x -axis, the sidebands in the positive x -axis all

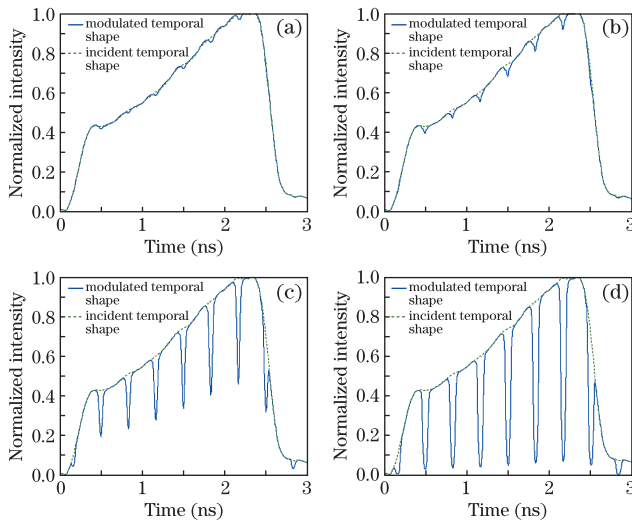


Fig. 6. Temporal shapes of input and output beams under various off-axis distances of (a) 52, (b) 104, (c) 156, and (d) 208 μm .

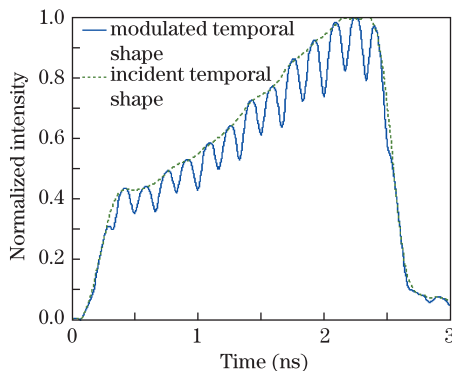


Fig. 7. FM-to-AM conversion under 10-mm defocus distance.

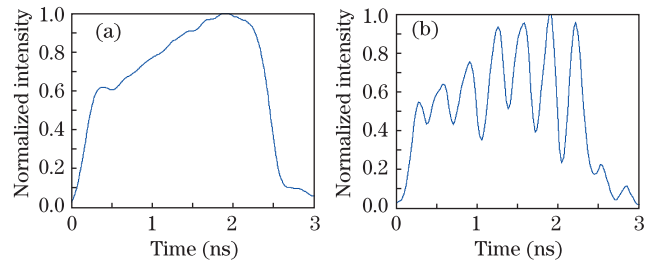


Fig. 8. FM-to-AM conversion measured in the experiment. (a) Injected pulse and (b) output pulse.

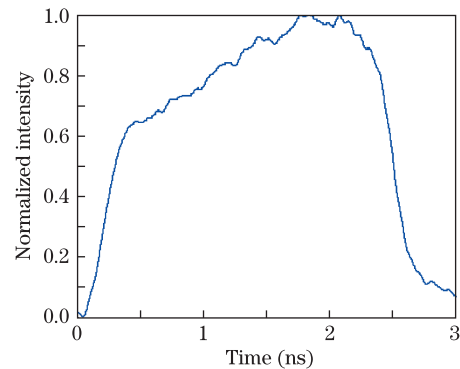


Fig. 9. Temporal shape with a modified pinhole.

pass through the pinhole, whereas sidebands in the negative x -axis are partially cut off. The same situation occurs in the y -axis. Because of the asymmetry of spectrum modulation is $fc \neq 0$, as mentioned in Eq. (4), modulation period is 0.33 ns, which is the same as the phase modulation. With the development of the off-axis distance, the distortion criterion increases.

The discussion above shows that only high-frequency components are cut off on the condition of different sizes of aperture. When the pinhole is not located at the focal plane, part of the beam might be cut off, and different spectral components have different intercepting factors related to the defocus distance. The central frequency has a low intercepting factor, whereas the high-frequency component has a high intercepting factor. This is a similar mathematical model to the case induced by gain narrowing^[12].

As shown in Fig. 7, the intensity modulation period is half of that of phase modulation because of the symmetry of intensity filtering function.

We measured the temporal shape in the SSD experiment. Figure 8(a) shows the waveform without phase modulation, whereas, in Fig. 8(b), as the phase of field is modulated, a severe FM-to-AM conversion occurs and the intensity modulation period is the same as the phase modulation period. This situation is similar to that in Fig. 6, in which pinhole central position is off-axis. After checking the filter pinhole, a breakdown at one side of the laser was found.

We then modified the pinhole central position and measured the temporal shape. As shown in Fig. 9, FM-to-AM conversion did not occur, and the waveform is almost the same as the one without modulation shown in Fig. 8(a).

In conclusion, the high-power laser system, phase modulation is required for SSD in order to improve the focal spot uniformity. Grating broadens the spectrum of optical field, thereby significantly affecting the design of the spatial filter. A pinhole with an insufficient size, off-axis, and defocused plane would result in a spectrum distortion, thereby causing FM-to-AM conversion. Because the temporal shape characteristics corresponding to the above three conditions are distinct, a detailed analysis on these characteristics is carried to diagnose the spatial filter system and design the pinhole parameter. An obvious FM-to-AM conversion occurred in the SSD experiment, and the modification based on the above analysis is implemented to solve this problem.

References

1. J. E. Rothenberg, D. F. Browning, and R. B. Wilcox, in *Proceedings of Third International Conference on Solid State Lasers for Application to Inertial Confinement Fusion*, Pts 1 and 2, 3492, 51 (1999).
2. J. R. Murray, J. R. Smith, R. B. Ehrlich, D. T. Kyrazis, C. E. Thompson, T. L. Weiland, and R. B. Wilcox, *J. Opt. Soc. Am. B: Opt. Phys.* **6**, 2402 (1989).
3. S. Skupsky and K. Lee, *J. Appl. Phys.* **54**, 3662 (1983).
4. S. Skupsky, R. W. Short, T. Craxton, S. Letzring, and J. M. J. Soures, *Appl. Phys.* **66**, 3456 (1989).
5. S. Hocquet, E. Bordenave, and D. Penninckx, in *Proceedings of 5th International Conference on Inertial Fusion Sciences and Applications* 112 (2008).
6. S. Hocquet, D. Penninckx, E. Bordenave, C. Gouard, and Y. Jaouën, *Appl. Opt.* **47**, 3338 (2008).
7. Y. Yang, S. B. Feng, W. Han, W. G. Zheng, F. Q. Li, and J. C. Tan, *Opt. Lett.* **34**, 3848 (2009).
8. A. Babushkin, W. Bittle, S. A. Letzring, M. D. Skeldon, and W. Seka, *Proc. SPIE* **3492**, 124 (1999).
9. D. Penninckx, N. Beck, J. Gleyze, and L. Videau, *J. Lightwave Technol.* **24**, 4197 (2006).
10. G. P. Agrawal, *Nonlinear Fiber Optics* (Academic Press, San Diego, 2001).
11. J. Li, H. Zhang, S. Zhou, W. Feng, J. Zhu, and Z. Lin, *Acta Opt. Sin.* (in Chinese) **30**, 827 (2010).
12. L. J. Waxer, J. H. Kelly, J. Rothenberg, A. Babushkin, C. Bibeau, A. Bayramian, and S. Payne, *Opt. Lett.* **27**, 1427 (2002).